Journal of Sound and Vibration (2000) **234**(1), 85–114
doi:10.1006/jsvi.1999.2860, available online at http://www.idealibrary.com on IDEAL®

ANALYTICAL METHODS OF DECOUPLING THE AUTOMOTIVE ENGINE TORQUE ROLL AXIS

TAESEOK JEONG AND RAJENDRA SINGH

Acoustics and Dynamics Laboratory, Department of Mechanical Engineering and, The Center for Automotive Research, The Ohio State University, Columbus, Ohio 43210-1107, *U.S.A.*

(*Received* 9 *July* 1999, *and in final form* 1 *December* 1999)

This paper analytically examines the multi-dimensional mounting schemes of an automotive engine–gearbox system when excited by oscillating torques. In particular, the issue of torque roll axis decoupling is analyzed in significant detail since it is poorly understood. New dynamic decoupling axioms are presented an d compared with the conventional elastic axis mounting and focalization methods. A linear time-invariant system assumption is made in addition to a proportionally damped system. Only rigid-body modes of the powertrain are considered and the chassis elements are assumed to be rigid. Several simplified physical systems are considered and new closed-form solutions for symmetric and asymmetric engine-mounting systems are developed. These clearly explain the design concepts for the 4-point mounting scheme. Our analytical solutions match with the existing design formulations that are only applicable to symmetric geometries. Spectra for all six rigid-body motions are predicted using the alternate decoupling methods and the closed-form solutions are verified. Also, our method is validated by comparing modal solutions with prior experimental and analytical studies. Parametric design studies are carried out to illustrate the methodology. Chief contributions of this research include the development of new or refined analytical models and closed-form solutions along with improved design strategies for the torque roll axis decoupling.

1. INTRODUCTION

There is considerable interest in controlling the automotive powertrain vibration problems through proper design of the rubber and hydraulic mounting systems [1–15]. The pulsating torque generated by the multi-cylinder engines is one of the major sources of vibration. This becomes even more critical in future vehicles which will employ high power density powertrains with lighter and more compact body frames. Mathematical models of the engine-mounting systems are therefore needed to fully understand the dynamic design issues, given increasingly stringent packaging and geometric constraints. This article analytically examines the three-dimensional mounting schemes that may dynamically decouple the torque roll axis (TRA).

The TRA is defined as an axis around which rotation occurs when a torque is exerted on a free rigid body about an arbitrary direction, say x in Figure 1(a). Since the system of Figure 1(a) is unconstrained, the TRA is determined by the inertial properties of the powertrain and the direction of the torque. It should be noted that the direction of the TRA may not be unique when it is purely defined by using the Euler's equations of motion for a free rigid body. Now assume that the system is constrained and the rotational displacements of the rigid body undergoing oscillations are small. Therefore, all second order terms in the Euler's equations of motion will be negligible and this will result in the unique TRA direction. In many practical cases, the TRA does not coincide with any of the

0022-460X/00/260085 + 30 $35.00/0

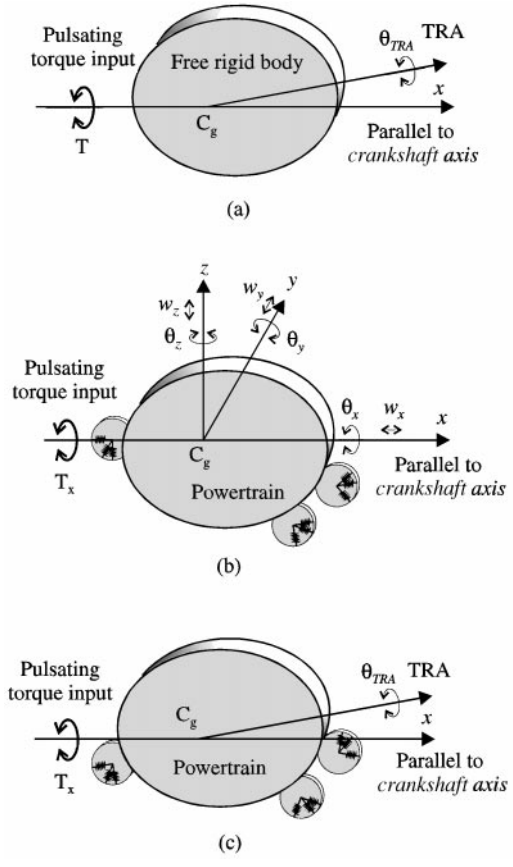

Figure 1. Schematic view of the torque roll axis (TRA) mode and decoupling concepts: (a) TRA for a free rigid body, (b) coupled powertrain mount system, (c) TRA mode-decoupled system.

principal inertial axes or the crankshaft axis [4–6]; in fact typical deviations may be up to 25°. When the powertrain is supported by multiple mounts, there exists six physical modes such as vertical bounce (w_z), longitudinal force-aft (w_x), horizontal side motion (w_y), roll (θ_x), pitch (θ_y), and yaw (θ_z) modes as shown in Figure 1(b). Now suppose that a torque T_x is applied about the x-axis, as defined by the reference co-ordinate system of Figure 1(b).

Two types of forced vibration responses may be produced. One is the pure rotational response about only the x-axis; designate it as the roll mode that is "decoupled" from the other physical modes. The second one is the coupled response along or about several axes; the roll mode is now "coupled" with the other physical modes. Some caution must be exercised regarding the terminology that is used in this area, especially with terms such as "coupling", "decoupling" and "mode". The term "mode" may refer to the forced response "mode" along or about a chosen physical co-ordinate axis. Hence, the term "physical mode" is adopted here instead of simply "mode" in order to differentiate it from the natural mode of vibration. Consequently, some of the terminology used before in the literature such as the "three coupled natural modes" [7] should be changed to the "three coupled physical modes" to avoid confusion.

2. TORQUE ROLL AXIS DECOUPLING CONCEPTS

Most dynamic design principles attempt to place the natural frequencies of the system below and above the excitation frequency range [8, 9]. However, if a system has several resonances within a narrow band, it becomes a rather difficult task to achieve. Therefore, a physically decoupled system has a better chance of producing fewer resonances over the operating range. For example, if a system is completely decoupled in physical modes, excitation along one physical co-ordinate should excite only one mode, as shown in Figure 1(c). Even when two or three different excitations are simultaneously applied to the powertrain, projected excitations along the physical co-ordinates may have only a few non-trivial values. Hence, physical decoupling of the powertrain is often necessary to ensure that vibro-acoustic performance goals will be achieved. Concurrently the mounting system must also satisfy the packaging needs, geometric constraints and static load-bearing requirements.

The elastic axis decoupling scheme is frequently a starting point in the industrial mounting system design practice [2, 6, 7, 10]. Elastic axes for an elastically supported rigid-body system are those axes along which only the displacement (or rotation), collinear with the direction of the applied static force (or moment), occurs as shown in Figure 2(a) and 2(b). If a physical co-ordinate system can be defined using elastic axes Γ_e and if it coincides with the principal inertial co-ordinate system Γ_p, the dynamic response consists of three decoupled translational and three rotational modes as shown in Figure 2(c). System mass and stiffness matrices are then diagonal either in Γ_p or Γ_e co-ordinates. However, Kim [11] maintains that the elastic center of mounts cannot always exist in a full three-dimensional (3-D) rigid-body system since only the six off-diagonal terms are forced to vanish in the physical domain. Therefore, the complete decoupling of a practical powertrain by the elastic axis mounting concept is impossible to achieve when one considers the 3-D asymmetric shape of the inertial body and arbitrary placement of the mounts. Consequently, the focalization method, which is related to the elastic axis decoupling concept, has been implemented as it partially decouples a system [2, 7]. Direct design methods of the mounting system also have been tried, using optimization algorithms, regardless of the coupling of physical modes. Bernard and Starkey [8] and Spiekermann *et al.* [9] applied optimization algorithms to prevent the resonances of the engine natural rigid-body mode from being excited by engine excitation. Ashrafiuon attempted to minimize the forces transmitted from the engine to the nacelle in an aircraft [14].

The true TRA mode decoupling strategy has also been sought by designers and researchers over the past two decades [4–6]. Requirements for the existence of a decoupled TRA mode are suggested by Geck and Patton [5] and these have been implemented in a numerical optimization scheme. But they could not obtain a more complete decoupling of the TRA mode. The TRA decoupling mechanisms therefore remain poorly understood and inadequately analyzed. New or refined dynamic decoupling conditions are obviously needed and these will be examined in this paper.

3. PROBLEM FORMULATION

Consider the generic powertrain system of Figure 3(a). Several approximations and simplifications must be made to establish a tractable research problem. These include the following. (1) Displacements of the powertrain are small. (2) The powertrain is represented by a rigid body of time-invariant inertial matrix **M** of dimension 6. (3) The powertrain is supported at four discrete locations as shown in Figure 5; rubber or hydraulic mounts are

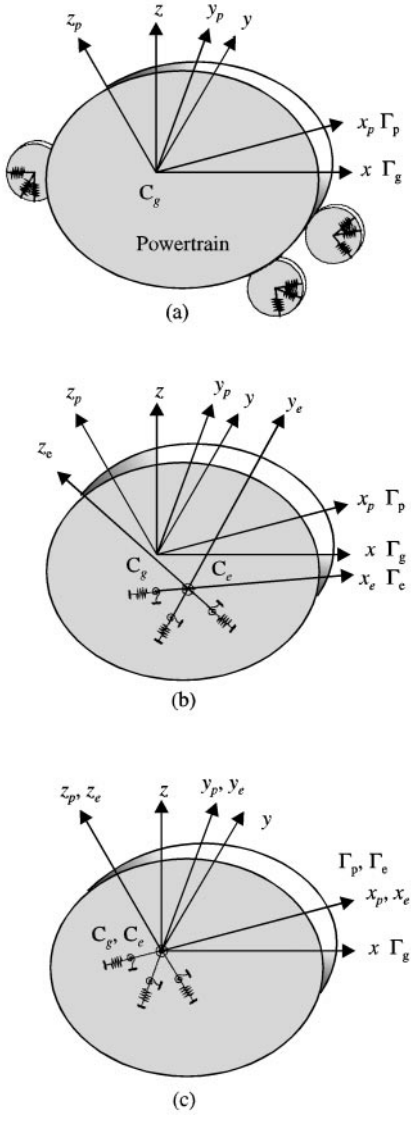

Figure 2. Elastic axis decoupling scheme and relevant coordinate systems. (a) A powertrain mount system with Γ_g (x, y, z) and Γ_p (x_p, y_p, z_p) co-ordinate systems. Here, C_g is the center of gravity. (b) Equivalent system representation in the elastic axis co-ordinate system Γ_e (x_e, y_e, z_e) when C_e is the elastic center. (c) Elastic axis decoupled system.

represented by tri-axial linear spring elements (k_p, k_q, and k_r). (4) Viscous **C** and/or structural **H** damping matrices are assumed to be known; they may be estimated from known modal damping ratios assuming a proportionally damped system. (5) The vehicle chassis may be modeled as a rigid termination. (6) The excitation is assumed to be either harmonic or periodic of known frequencies, amplitudes, and phases. (7) Emphasis is initially placed on the lower frequencies (up to 50 Hz) covering six modes of rigid-body vibration; the upper-frequency range may be extended in future work when the relevant vehicle chassis and powertrain vibrational responses are included.

For the generic powertrain mount system of Figure 3(b), the inertial co-ordinate system for the rigid body is denoted as Γ_g, the TRA co-ordinate system is given by Γ_{TRA}, and the

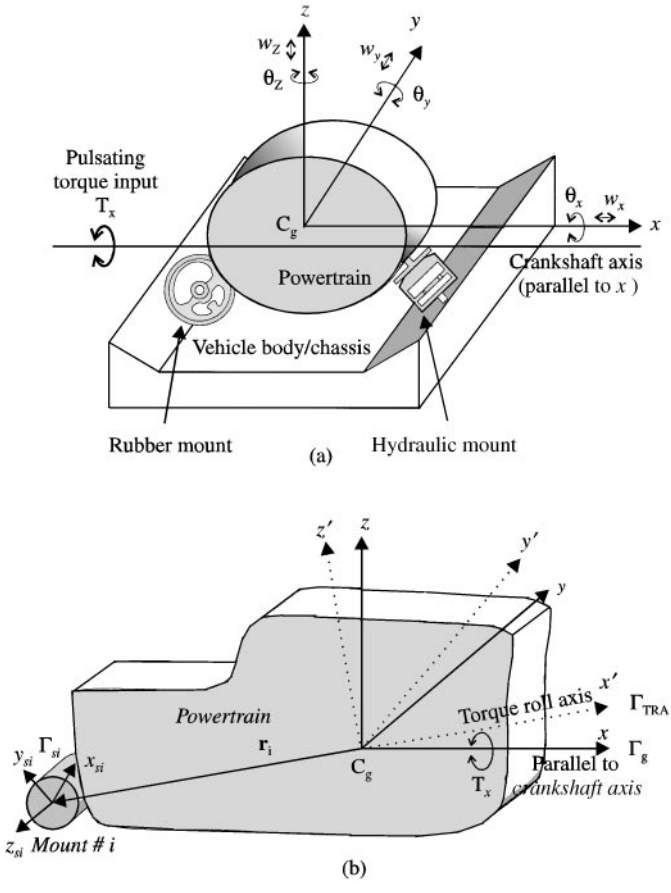

Figure 3. Physical system of interest. (a) A generic powertrain with rubber and/or hydraulic mounts. Only pulsating torque excitation is illustrated here. (b) Co-ordinate systems $\Gamma_g\,(x, y, z)$, $\Gamma_{TRA}\,(x', y', z')$, and $\Gamma_{si}\,(x_{si}, y_{si}, z_{si})$.

principal elastic co-ordinate system of the ith mount is defined by Γ_{si}. The crankshaft axis is parallel to the x direction in Γ_g and the TRA is parallel to the x' direction in Γ_{TRA}. The position vector $\mathbf{r}_i = [a_{xi}\ a_{yi}\ a_{zi}]^{\mathrm{T}}$ of the ith mount is in the Γ_g system. A generalized co-ordinate vector $\mathbf{q}$ is defined by combining translations ($\mathbf{w}_g$) and rotational ($\boldsymbol{\theta}_g$) displacements of the powertrain center of gravity ($\mathbf{C}_g$):

$$\mathbf{q} = [\mathbf{w}_g^{\mathrm{T}}, \boldsymbol{\theta}_g^{\mathrm{T}}]^{\mathrm{T}} = [[w_x\ \ w_y\ \ w_z], [\theta_x\ \ \theta_y\ \ \theta_z]]^{\mathrm{T}}. \tag{1}$$

Specific objectives of this article are as follows. (1) Develop an analytical formulation of the problem and derive mathematical conditions that yield a more complete dynamic decoupling of the torque roll axis mode by proposing a new axiom. (2) Compare the proposed dynamic decoupling technique with the existing elastic axis mounting design and focalization methods. (3) Obtain closed-form solutions for a few simplified mounting schemes to better understand the effect of mounting parameters. (4) Compare various methods and validate the proposed formulation by comparing modal solutions with those given by Spiekermann *et al.* [9].

4. ANALYTICAL MODEL

The inertia matrix $\mathbf{M}$ of the powertrain (engine and gearbox) consists of the following translational ($\mathbf{M}_w$) and rotational ($\mathbf{M}_\theta$) inertia terms, where m is the system mass, I is the moment of inertia, and *diag* implies a diagonal matrix (also refer to Appendix A for the identification of symbols):

$$\mathbf{M} = \begin{bmatrix} \mathbf{M}_w & \mathbf{0} \\ \mathbf{0} & \mathbf{M}_\theta \end{bmatrix}, \quad \mathbf{M}_w = diag([m \;\; m \;\; m]), \quad \mathbf{M}_\theta = \begin{bmatrix} I_{xx} & -I_{xy} & -I_{xz} \\ -I_{xy} & I_{yy} & -I_{yz} \\ -I_{xz} & -I_{yz} & I_{zz} \end{bmatrix}. \tag{2}$$

Inertial properties may be estimated based on simplified powertrain geometry or from solid models/finite element analyses. The mounting system stiffness matrix $\mathbf{K}$ can be obtained by considering the reaction forces and moments from mounts when the center of gravity $\mathbf{C}_g$ is displaced. Consider the planar rigid-body powertrain of Figure 4 where only the translations along x and y directions and the rotation (θ_z) around the z axis are considered [7]. The torque reaction from mounts due to θ_z will be $(k_t + a_y^2 k_x)\theta_z$. If k_t is assumed to be of the same order of magnitude as $r_c^2 k_x$, where r_c is a characteristic dimension of a mount, we obtain the following relationship: $k_t/a_y^2 k_x \approx (r_c/a_y)^2$. Values of r_c/a_y for a typical rubber mount range from 0.1 to 0.2, and therefore the contribution of k_t is negligible. Consequently, the stiffness matrix of the ith mount $\mathbf{K}_{si}$ in Γ_{si} may be simplified as

$$\mathbf{K}_{si} = diag([k_{pi} \;\; k_{qi} \;\; k_{ri}]), \tag{3}$$

where k_p is the principal compressive stiffness, and k_q and k_r are the principal shear stiffnesses. A transformation matrix $\mathfrak{R}_{g,si}$ between Γ_g and Γ_{si} co-ordinates is used to obtain the static stiffness matrix $\mathbf{K}_{gi}$ of the ith mount in Γ_g from $\mathbf{K}_{si}$. The elements of $\mathfrak{R}_{g,si}$ consist of directional cosines of Γ_{si} with respect to Γ_g since only the rotational transformation must be considered. The matrix $\mathbf{K}_{gi}$ is obtained as

$$\mathbf{K}_{gi} = \mathfrak{R}_{g,si}\mathbf{K}_{si}\mathfrak{R}_{g,si}^{\mathrm{T}} = \begin{bmatrix} k_{xxi} & k_{xyi} & k_{xzi} \\ k_{xyi} & k_{yyi} & k_{yzi} \\ k_{xzi} & k_{yzi} & k_{zzi} \end{bmatrix}. \tag{4}$$

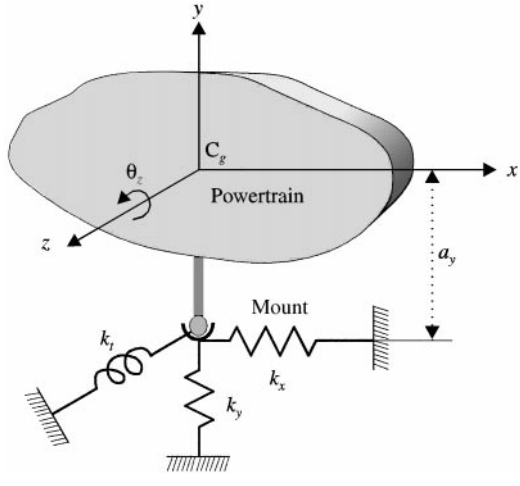

Figure 4. Consideration of torsional stiffness k_t in a powertrain mount.

Let $\mathbf{w}_i$ be the deflection vector for the ith mount,

$$\mathbf{w}_i = \mathbf{w}_g + \boldsymbol{\theta}_g \times \mathbf{r}_i. \tag{5}$$

Instead, we use the rotation matrix $\mathbf{B}_i$ for the cross-vector product and rewrite equation (5) as follows where $\mathbf{I}$ is an identity matrix of dimension 3:

$$\mathbf{w}_i = [\mathbf{I} \;\; \mathbf{B}_i^{\mathrm{T}}]\mathbf{q}, \quad \mathbf{B}_i = \begin{bmatrix} 0 & -a_{zi} & a_{yi} \\ a_{zi} & 0 & -a_{xi} \\ -a_{yi} & a_{xi} & 0 \end{bmatrix}. \tag{6, 7}$$

The translational reaction force $\mathbf{R}_{wi}$ and moment reaction $\mathbf{R}_{\theta i}$ from the ith mount are

$$\mathbf{R}_{wi} = -\mathbf{K}_{gi}\mathbf{w}_i = -\mathbf{K}_{gi}[\mathbf{I} \;\; \mathbf{B}^{\mathrm{T}}]\mathbf{q}, \tag{8}$$

$$\mathbf{R}_{\theta i} = \mathbf{r}_i \times \mathbf{R}_{wi} = \mathbf{B}_i\mathbf{R}_{wi} = -\mathbf{B}_i\mathbf{K}_{gi}[\mathbf{I} \;\; \mathbf{B}^{\mathrm{T}}]\mathbf{q}. \tag{9}$$

Combining reaction force and moment, one obtains the reaction vector

$$\begin{bmatrix} \mathbf{R}_{wi} \\ \mathbf{R}_{\theta i} \end{bmatrix} = -\begin{bmatrix} \mathbf{K}_{gi} & \mathbf{K}_{gi}\mathbf{B}_i^{\mathrm{T}} \\ (\mathbf{K}_{gi}\mathbf{B}_i^{\mathrm{T}})^{\mathrm{T}} & \mathbf{B}_i\mathbf{K}_{gi}\mathbf{B}_i^{\mathrm{T}} \end{bmatrix}\mathbf{q}. \tag{10}$$

Hence, the contribution of all mounts to the system stiffness matrix may be combined and expressed as follows, where both $\mathbf{K}_i$ and $\mathbf{K}$ are square matrices of dimension 6 and i is the mount index:

$$\mathbf{K} = \sum_{i=1}^{n} \mathbf{K}_i = \sum_{i=1}^{n} \begin{bmatrix} \mathbf{K}_{gi} & \mathbf{K}_{gi}\mathbf{B}_i^{\mathrm{T}} \\ (\mathbf{K}_{gi}\mathbf{B}_i^{\mathrm{T}})^{\mathrm{T}} & \mathbf{B}_i\mathbf{K}_{gi}\mathbf{B}_i^{\mathrm{T}} \end{bmatrix}. \tag{11}$$

Using equation (2) and (11) we can construct the governing equations of the LTI system in matrix form as follows where only small oscillations are assumed in addition to linear system parameters:

$$\mathbf{M}\ddot{\mathbf{q}}(t) + \mathbf{C}\dot{\mathbf{q}}(t) + \mathbf{K}\mathbf{q}(t) = \mathbf{f}(t), \tag{12}$$

where $\mathbf{f}$ is the external force vector and $\mathbf{C}$ is the viscous damping matrix assuming a proportionally damped system. Note that the mean load and torque terms are deleted and hence the generalized vector $\mathbf{q}$ represents perturbations about the static equilibrium. Mean rotation is ignored as well. Structural damping may also be included by replacing $\mathbf{C}\dot{\mathbf{q}}(t)$ by $\mathrm{i}\mathbf{H}\mathbf{q}(t)$, where $\mathrm{i} = \sqrt{-1}$, but this formulation is valid in the frequency domain only.

5. TORQUE ROLL AXIS DECOUPLING AXIOMS

Geck and Patton [5] have stated the following two axioms and provided the necessary mathematical proofs regarding the TRA mode decoupling, by assuming the powertrain mounting system is given an undamped LTI system formulation. These are rephrased using

our notation. Refer to Appendix B for a more mathematical definition of the TRA direction $\mathbf{q}_{TRA}$.

1. *The torque pulses $T(t)$ will excite one and only one mode if and only if the mode shape of that mode is a rotation around the torque roll axis.*
2. *A system has a mode about the torque roll axis if and only if $\mathbf{K}\mathbf{q}_{TRA}$ is parallel to $\mathbf{T}$ where $\mathbf{K}$ is the stiffness matrix for the system, $\mathbf{q}_{TRA}$ is the normalized TRA direction and $\mathbf{T}$ is oscillating torque.*

We may conclude from the above statements that if the TRA direction coincides with one of the natural modes of vibration, i.e., the natural mode of vibration is solely a rigid-body rotation, then the response will be a rotation around the TRA regardless of the excitation frequency. Note that the response has a constant direction since the TRA depends only on the time-invariant inertial properties and the direction of the applied torque which also has a fixed direction. The following two questions may be raised in criticism to the above because one may question if the TRA mode decoupling is the only method of obtaining a constant directional response.

(a) If the response to a torque has a constant rotational direction, should it be a rotation around the TRA?
(b) If the response to a torque is a pure rotation around the TRA, should it belong to one of the natural modes of vibration?

To answer the above, we propose a new axiom, designated below as 3.

3. *If a rigid-body system excited by a force (torque or moment) with a constant direction responds in a constant translational (rotational) direction and varies only with the excitation frequency, then that response must be one of the natural modes of vibration.*

The proof of axiom 3 is given next. Assume, without loss of generality, that a powertrain mounting system is linear and undamped. Also assume that system matrices of dimension N are positive definite, and that excitation is harmonic at frequency ω. Distinct natural frequencies (ω_r) and eigenvectors ($\mathbf{u}_r$) are also assumed here, where $\mathbf{r}$ is the modal index. Define harmonic force $\mathbf{f}(t) = a(\omega)\mathbf{f}_a e^{i\omega t}$ and response $\mathbf{q}(t) = b(\omega)\mathbf{q}_a e^{i\omega t}$ vectors where a and b are spectrally varying scalar functions, and $\mathbf{f}_a$ and $\mathbf{q}_a$ are frequency-invariant amplitude vectors. By using the modal expansion theorem, the response is as expressed.

$$b(\omega)\mathbf{q}_a = \sum_{r=1}^{N} c_r(\omega)\mathbf{u}_r, \tag{13}$$

where c_r is scalar and a function of ω and it may be called the modal participation factor. Since all eigenvectors are linearly independent of each other, they form a basis for the real vector space of dimension N. Hence $\mathbf{q}_a$ is expressed as

$$\mathbf{q}_a = \sum_{r=1}^{N} d_r\mathbf{u}_r, \tag{14}$$

where d_r is a scalar constant. Since the response is non-trivial, at least one of the scalar coefficients in equation (14) should not be zero. Assume that $d_j \neq 0$. Substituting equation (14) into equation (13) and rearranging, obtain

$$\mathbf{0} = (c_1(\omega) - d_1 b(\omega))\mathbf{u}_1 + \cdots + (c_r(\omega) - d_r b(\omega))\mathbf{u}_r + \cdots + (c_N(\omega) - d_N b(\omega))\mathbf{u}_N. \tag{15}$$

Since the $\mathbf{u}_r$'s are independent of each other, $c_r(\omega)$ equals to $d_r b(\omega)$, where $b(\omega)$ equals to $c_j(\omega)/d_j$ from the jth term. Hence d_r $(r = 1, \ldots, N;\ r \neq j)$ is expressed as

$$d_r = d_j \frac{c_r(\omega)}{c_j(\omega)}. \tag{16}$$

The relationship (16) should be valid at all frequencies. Choose a case when the excitation ω approaches the jth natural frequency ω_j,

$$\lim_{\omega \to \omega_j} d_r = \lim_{\omega \to \omega_j} \left[d_j \frac{c_r(\omega)}{c_j(\omega)} \right] = 0. \tag{17}$$

Therefore, we can conclude that all d_r's are zero unless $r = j$, meaning that $\mathbf{f}_a$ is parallel to $\mathbf{u}_j$ and it is also one of the natural modes. This completes the proof.

The axiom 3 can now answer the two questions that were posed previously. For question (a), when the constant direction of the response becomes a natural mode of the system by axiom 3, then it should be a rotation around the TRA per axiom 1. Regarding question (b), since the response is a rotation around the TRA, it has a constant direction. Hence it should belong to the natural modes by axiom 3. Therefore, the TRA mode decoupling is the only way to achieve a constant directional response. A complete dynamic decoupling of the TRA mode depends solely now on whether a natural mode can be forced to be in the TRA direction or not. In general, a constant directional response may be obtained for any arbitrary force input with a constant direction. For example, if a dynamic force is vertically applied at C_g, there exists an axis along which the response occurs as a free rigid body. Similar to the TRA mode decoupling, a complete or partial decoupling of other physical modes may also be obtained; this goal is left for future research.

6. DYNAMIC DECOUPLING METHOD

6.1. ANALYTICAL FORMULATION

A more general mathematical condition for a complete decoupling can be obtained in the TRA co-ordinate system where TRA is one of the axes. Define a transformation from co-ordinate system Γ_g to co-ordinate system Γ_{TRA}. Start with the following undamped equations of motion for a powertrain mounting system:

$$\mathbf{M}\ddot{\mathbf{q}}(t) + \mathbf{K}\mathbf{q}(t) = \mathbf{f}(t), \tag{18}$$

where $\mathbf{M}$ is defined by equation (2) and $\mathbf{K}$ by equation (11). Define the following relationship where a is a normalizing constant for the first column of matrix:

$$\mathbf{J} = a \begin{bmatrix} J_{11} & J_{12} & J_{13} \\ J_{21} & J_{22} & J_{23} \\ J_{31} & J_{32} & J_{33} \end{bmatrix} = \begin{bmatrix} I_{xx} & -I_{xy} & -I_{xz} \\ -I_{xy} & I_{yy} & -I_{yz} \\ -I_{xz} & -I_{yz} & I_{zz} \end{bmatrix}^{-1}. \tag{19}$$

Assume that a harmonic torque is applied about the x-axis. Using equations (B2) and (B3), the TRA direction is defined as

$$\mathbf{q}_{TRA} = [0\ \ 0\ \ 0\ \ J_{11}\ \ J_{21}\ \ J_{31}]^{\mathrm{T}}. \tag{20}$$

Formulate a new co-ordinate system where the x' direction is parallel to $\mathbf{q}_{TRA}$ and the origin is located on the center of gravity C_g of the powertrain. The directional cosine vector between x' and the original co-ordinate system (x, y, z) is obtained as

$$[v_{x'x} \;\; v_{x'y} \;\; v_{x'z}] = [J_{11} \;\; J_{21} \;\; J_{31}]. \tag{21}$$

The directional cosine vectors for y' and z' directions may be chosen arbitrary as long as the following equation is valid and the resulting transformation matrix is orthonormal. Any orthonormal vectors lying on the following plane that is defined in Γ_g can be used as the directional cosine vectors for them:

$$J_{11}x + J_{21}y + J_{31}z = 0. \tag{22}$$

Similarly, the directional cosine vectors for y' and z' may be defined as

$$[v_{y'x} \;\; v_{y'y} \;\; v_{y'z}] = \frac{[v_{y'x0} \;\; v_{y'y0} \;\; v_{y'z0}]}{|[v_{y'x0} \;\; v_{y'y0} \;\; v_{y'z0}]|}; \quad [v_{z'x} \;\; v_{z'y} \;\; v_{z'z}] = \frac{[v_{z'x0} \;\; v_{z'y0} \;\; v_{z'z0}]}{|[v_{z'x0} \;\; v_{z'y0} \;\; v_{z'z0}]|}, \tag{23}$$

where $v_{y'y0}$, $v_{y'z0}$, and $v_{z'z0}$ may assume any arbitrary values and

$$v_{y'x0} = -\frac{J_{21}v_{y'y0} + J_{31}v_{y'z0}}{J_{11}}; \quad \begin{bmatrix} v_{z'x0} \\ v_{z'y0} \end{bmatrix} = -\begin{bmatrix} J_{11} & J_{21} \\ v_{y'x} & v_{y'y} \end{bmatrix}^{-1} \begin{bmatrix} J_{31} \\ v_{y'z} \end{bmatrix} v_{z'z0}. \tag{24}$$

Designate this as the orthonormal transformation matrix $\mathfrak{R}_{g',g}$:

$$\mathfrak{R}_{g',g} = \begin{bmatrix} v_{x'x} & v_{x'y} & v_{x'z} \\ v_{y'x} & v_{y'y} & v_{y'z} \\ v_{z'x} & v_{z'y} & v_{z'z} \end{bmatrix}, \tag{25}$$

where the entire row vectors are defined by equations (21) and (23). Define the transformation matrix, $\mathbf{\Pi}_{g',g}$ of dimension 6 as

$$\mathbf{\Pi}_{g',g} = \begin{bmatrix} \mathfrak{R}_{g',g} & \mathbf{0} \\ \mathbf{0} & \mathfrak{R}_{g',g} \end{bmatrix}. \tag{26}$$

The undamped governing equation of motion in the TRA co-ordinate system is defined as

$$\mathbf{M}'\ddot{\mathbf{q}}'(t) + \mathbf{K}'\mathbf{q}'(t) = \mathbf{f}'(t), \tag{27}$$

$$\mathbf{M}' = \mathbf{\Pi}_{g',g}\mathbf{M}\mathbf{\Pi}_{g',g}^{\mathrm{T}}, \quad \mathbf{K}' = \mathbf{\Pi}_{g',g}\mathbf{K}\mathbf{\Pi}_{g',g}^{\mathrm{T}}, \mathbf{f}' = \mathbf{\Pi}_{g',g}\mathbf{f}. \tag{28}$$

6.2. CONDITIONS FOR DECOUPLING THE TORQUE ROLL AXIS MODE

All equations in this section are defined in the TRA co-ordinate system (x', y', z'). However, the superscript used to denote the TRA coordinate system is dropped here for the sake of convenience. To achieve a complete decoupling of the TRA mode from other physical modes, the TRA direction $\mathbf{q}_{TRA} = [0 \;\; 0 \;\; 0 \;\; 1 \;\; 0 \;\; 0]^{\mathrm{T}}$ should be one of natural modes.

In other words, the $\mathbf{Kq}_{TRA} = \lambda \mathbf{Mq}_{TRA}$ relationship should be satisfied where λ is the eigenvalue. Expressed in detail,

$$\sum_{i=1}^{n} (k_{xzi} a_{yi} - k_{xyi} a_{zi}) = 0, \quad \sum_{i=1}^{n} (k_{yzi} a_{yi} - k_{yyi} a_{zi}) = 0, \quad \sum_{i=1}^{n} (k_{zzi} a_{yi} - k_{yzi} a_{zi}) = 0, \quad (29a\text{–}c)$$

$$\sum_{i=1}^{n} (k_{yyi} a_{zi}^2 + k_{zzi} a_{yi}^2 - 2k_{yzi} a_{yi} a_{zi}) = \lambda I_{xx}, \quad (29d)$$

$$\sum_{i=1}^{n} (k_{xzi} a_{yi} z_{zi} + k_{yzi} a_{xi} a_{zi} - k_{zzi} a_{xi} a_{yi} - k_{xyi} a_{zi}^2) = -\lambda I_{xy}, \quad (29e)$$

$$\sum_{i=1}^{n} (k_{xyi} a_{yi} a_{zi} + k_{yzi} a_{xi} a_{yi} - k_{yyi} a_{xi} a_{zi} - k_{xzi} a_{yi}^2) = -\lambda I_{xz}. \quad (29f)$$

These equations represent the conditions for a complete decoupling of the TRA mode. Since in equations are available, up to six mounting parameters may be adjusted. For example, one may vary three stiffness ratios and three orientation angles or even six location parameters while holding other parameters as constants.

7. ANALYTICAL SOLUTIONS FOR SIMPLIFIED MOUNTING SYSTEMS

Consider several simplified mounting systems, which are devised to obtain closed-form solutions to equation (29). Analytical results should reveal an understanding of the effect of mounting parameters, while providing a starting point for the dynamic design. The traditional mount-positioning scheme, as shown in Figure 5, is examined.

7.1. FOUR-POINT MOUNTING SYSTEM

A four-point simplified mounting system is shown in Figures 6 and 7. Note that the inertial system is not simplified here. Instead, the only simplification made here is to restrict the mounting orientations such that the compressive principal stiffness direction and one shear stiffness direction from each mount lie in the so-called mounting planes, which are parallel to the y–z plane. The TRA co-ordinate system is adopted and the proposed decoupling conditions will be employed. The origin of Γ_{si} in the mounting plane is specified in the two-dimensional mounting co-ordinate system Γ_{mi}. The origin of Γ_{mi} is located at point P_i whose co-ordinates are (p_{xi}, p_{yi}, p_{zi}) in Γ_{TRA}. Two system design parameters are orientation angle ϕ_i and mounting distance s_i; these are in Γ_{mi}. Assume that all four mounts are elastically identical, all orientation angles are equal to ϕ and the two mounting planes are located from C_g by the same distance a_x. Since two principal stiffness directions are parallel to the y–z plane, two cross-axis stiffness values, k_{xz} and k_{xy}, of each mount are zero; this assumption eliminates equation (29a). Define the relationship

$$k_y = k_p \sin^2 \phi + k_q \cos^2 \phi, \qquad k_z = k_p \cos^2 \phi + k_q \sin^2 \phi, \qquad k_{yz} = (k_p - k_q) \sin \phi \cos \phi. \quad (30a\text{–}c)$$

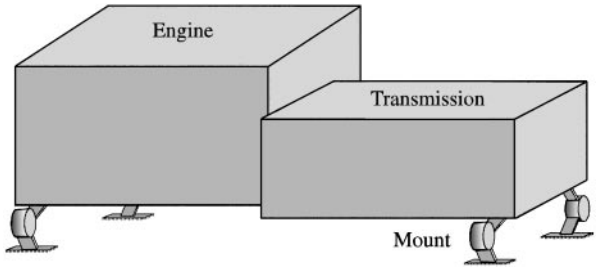

Figure 5. Four-point mount positioning scheme.

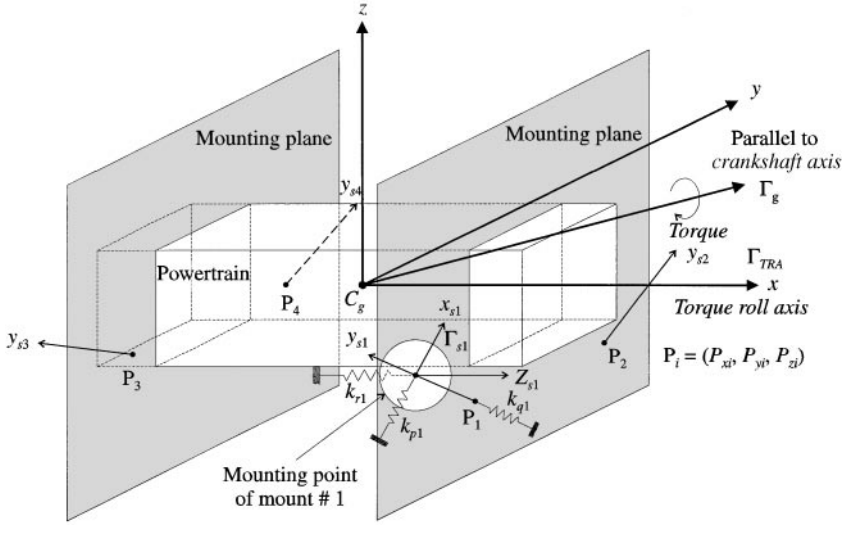

Figure 6. Simplified mounting scheme for an asymmetric powertrain.

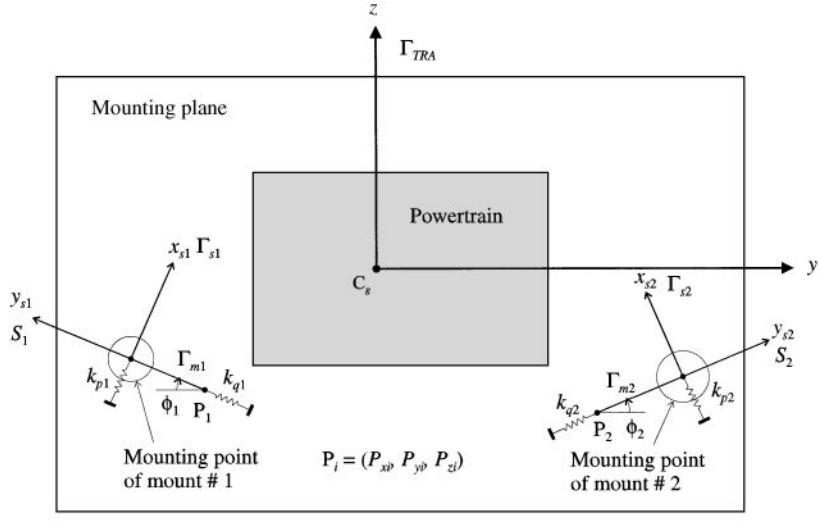

Figure 7. Scheme for the mounting plane.

Now express stiffnesses of each mount as

$$k_{yy1} = k_{yy2} = k_{yy3} = k_{yy4} = k_y, \quad k_{zz1} = k_{zz2} = k_{zz3} = k_{zz4} = k_z,$$

$$k_{yz1} = -k_{yz2} = k_{yz3} = -k_{yz4} = k_{yz}. \tag{31a–c}$$

Mount locations are defined as

$$a_{y1} = p_{y1} - s_1 \cos\phi, \quad a_{y2} = p_{y2} + s_2 \cos\phi, \quad a_{y3} = p_{y3} - s_3 \cos\phi,$$

$$a_{y4} = p_{y4} + s_4 \cos\phi, \quad a_{z1} = p_{z1} + s_1 \sin\phi, \quad a_{z2} = p_{z2} + s_2 \sin\phi,$$

$$a_{z3} = p_{z3} + s_3 \sin\phi, \quad a_{z4} = p_{z4} + s_4 \sin\phi. \tag{32a–h}$$

Substituting equations (31) and (32) into equations (29b–d, f), and solving for s_i, one obtain

$$s_1 = \frac{1}{2N_1}\{k_{yz}(p_{y1} - p_{y2}) - k_y(p_{z1} + p_{z2})\} + \frac{1}{2N_2}\{k_z(p_{y1} + p_{y2}) - k_{yz}(p_{z1} - p_{z2})\} + \frac{\lambda}{4a_x}\left(\frac{I_{xz}}{N_1} - \frac{I_{xy}}{N_2}\right),$$

$$s_2 = \frac{1}{2N_1}\{k_{yz}(p_{y1} - p_{y2}) - k_y(p_{z1} + p_{z2})\} - \frac{1}{2N_2}\{k_z(p_{y1} + p_{y2}) - k_{yz}(p_{z1} - p_{z2})\} - \frac{\lambda}{4a_x}\left(\frac{I_{xz}}{N_1} + \frac{I_{xy}}{N_2}\right),$$

$$s_3 = \frac{1}{2N_1}\{k_{yz}(p_{y3} - p_{y4}) - k_y(p_{z3} + p_{z4})\} - \frac{1}{2N_2}\{k_z(p_{y3} + p_{y4}) - k_{yz}(p_{z3} - p_{z4})\} + \frac{\lambda}{4a_x}\left(\frac{I_{xz}}{N_1} - \frac{I_{xy}}{N_2}\right),$$

$$s_4 = \frac{1}{2N_1}\{k_{yz}(p_{y3} - p_{y4}) - k_y(p_{z3} + p_{z4})\} + \frac{1}{2N_2}\{k_z(p_{y3} + p_{y4}) - k_{yz}(p_{z3} - p_{z4})\} - \frac{\lambda}{4a_x}\left(\frac{I_{xz}}{N_1} + \frac{I_{xy}}{N_2}\right), \tag{33a–d}$$

where

$$N_1 = k_{yz}\cos\phi + \mathrm{k_y}\sin\phi = k_p \sin\phi, \quad N_2 = k_{yz}\sin\phi + k_z\cos\phi = k_p\cos\phi. \tag{33e, f}$$

A similar but rather lengthy expression is obtained from equation (29e)

$$\frac{\lambda I_{xx}}{k_p} = (s_1^2 + s_2^2 + s_3^2 + s_4^2) + 2(p_{z1}s_1 + p_{z2}s_2 + \ + p_{z3}s_3 + p_{z4}s_4)\sin\phi$$

$$- 2(p_{y1}s_1 - p_{y2}s_2 + p_{y3}s_3 - p_{y4}s_4)\cos\phi + (p_{z1}^2 + p_{z2}^2 + p_{z3}^2 + p_{z4}^2)\sin^2\phi$$

$$+ (p_{y1}^2 + p_{y2}^2 + p_{y3}^2 + p_{y4}^2)\cos^2\phi - 2(p_{y1}p_{z1} - p_{y2}p_{z2} + p_{y3}p_{z3} - p_{y4}p_{z4})\sin\phi\cos\phi$$

$$+ \frac{1}{L}\{(p_{z1}^2 + p_{z2}^2 + p_{z3}^2 + p_{z4}^2)\cos^2\phi + (p_{y1}^2 + p_{y2}^2 + p_{y3}^2 + p_{y4}^2)\sin^2\phi$$

$$+ 2(p_{y1}p_{z1} - p_{y2}p_{z2} + p_{y3}p_{z3} - p_{y4}p_{z4})\sin\phi\cos\phi\}. \tag{34}$$

Equations (33) and (34) are rather cumbersome to analyze. Therefore, consider two special cases to get more tractable closed-form solutions.

7.2. SYMMETRIC INERTIAL SYSTEM

Because of the physical symmetry of the powertrain, I_{xy} and I_{xz} of equation (2) are zero. Choose the origins of the mounting co-ordinates such that $p_{y1} = -p_{y2} = p_{y3} = -p_{y4} = -y_0 < 0$ and $p_{z1} = p_{z2} = p_{z3} = p_{z3} = p_{z3} - z_0 < 0$. Equation (33) is reduced as follows, where $L = k_p/k_q$ is the stiffness or rate ratio:

$$s_1 = s_2 = s_3 = s_4 = s_0 = (z_0\sin\phi - y_0\cos\phi) + \frac{\cos\phi}{L}(z_0\cot\phi + y_0). \tag{35}$$

Insert the above into equation (34) and obtain the following natural frequency for the decoupled TRA mode:

$$\lambda_{r0} = \omega_{r0}^2 = \frac{4k_p}{L^2 I_{xx}}\{(z_0\cos\phi\cot\phi + y_0\cos\phi)^2 + L(z_0\cos\phi + y_0\sin\phi)^2\}. \tag{36}$$

Combine equations (35) and (36) to yield the following results; this matches with the expression of reference [7]:

$$\lambda_{r0} = \omega_{r0}^2 = \frac{4k_p}{I_{xx}}\left\{\frac{(y_0 + s_0\cos\phi)^2}{\frac{1}{L}\sin^2\phi + \cos^2\phi}\right\}. \tag{37}$$

7.3. ASYMMETRIC INERTIAL SYSTEM

Again, choose the origins of the mounting co-ordinates such that

$$p_{z1} = p_{z2} = p_{z3} = p_{z3} = -z_0 < 0, \quad p_{y1} = p_{y3}, \quad p_{y2} = p_{y4}, \quad p_{y1} - p_{y2} = p_{y3} - p_{y4} = -2y_0 < 0,$$

and $p_{y1} + p_{y2} = p_{y3} + p_{y4} = 2\Delta y_0$. Due to the asymmetric nature, the s_i's are obtained as

$$s_0 = (z_0\sin\phi - y_0\cos\phi) + \frac{\cos\phi}{L}(z_0\cot\phi + y_0), \quad s_1 = s_0 + s_g + s_{I_{xz}} - s_{I_{xy}},$$

$$s_2 = s_0 - s_g + s_{I_{xz}} + s_{I_{xy}}, \quad s_3 = s_0 + s_g - s_{I_{xz}} + s_{I_{xy}}, \quad s_4 = s_0 - s_g - s_{I_{xz}} - s_{I_{xy}},$$

$$s_g = \Delta y\left(\cos\phi + \frac{1}{L}\sin\phi\tan\phi\right), \quad s_{I_{xz}} = \frac{\lambda I_{xz}}{4a_x k_p\sin\phi}, \quad s_{I_{xy}} = \frac{\lambda I_{xy}}{4a_x k_p\cos\phi}. \tag{38a–h}$$

Here, we may interpret s_g as a "correction factor" to s_0 due to a change in the C_g location along the y direction; $s_{I_{xz}}$ is due to the coupling moment of inertia I_{xz}, and $s_{I_{xy}}$ is due to I_{xy}. Using equation (38), the effect of asymmetry in achieving the TRA mode decoupling may be determined. When combined with equation (34), some mounting parameters for a complete decoupling may be obtained. Substituting equation (38) into equation (34), one obtains a second order polynomial of $\lambda = \omega_r^2$. The solution is

$$\omega_r^2 = \frac{2k_p a_x^2 \sin^2\phi}{I_{xx}(\gamma_z^2 + \gamma_y^2 \tan^2\phi)}(1 \pm \sqrt{1 - D}), \quad \gamma_y = \frac{I_{xy}}{I_{xx}}, \quad \gamma_z = \frac{I_{xz}}{I_{xx}},$$

$$D = \frac{4}{a_x^2 L^2}\left(\frac{\gamma_z^2}{\sin^2\phi} + \frac{\gamma_y^2}{\cos^2\phi}\right)\left\{\begin{matrix}(z_0 \cos\phi \cot\phi + y_0 \cos\phi)^2 + L(z_0 \cos\phi + y_0 \sin\phi)^2 \\ + \Delta y^2 \sin^2\phi(\tan^2\phi + L)\end{matrix}\right\}. \tag{39a–d}$$

From equation (39) one can determine whether a complete decoupling exists or not for a given mounting configuration; it is given by

$$D \leqslant 1 \tag{40}$$

The parametric study based on equation (40) will be discussed in section 9 where two numerical examples are presented that will confirm the closed-form solutions.

8. ELASTIC AXIS DECOUPLING AND FOCALIZATION METHODS

To achieve a decoupled powertrain system, the mounting system should be adjusted such that the elastic center C_e exists within the powertrain body. After statically adjusting the mounting system, one may try matching Γ_e to Γ_p. The mathematical interpretation of the elastic axis decoupling method is described next. When equation (12) is derived in Γ_p, the mass matrix **M** becomes diagonal. Elastic axis decoupling is now achieved by diagonalizing the stiffness matrix **K** in Γ_p through the proper selection of mount locations, orientations, and stiffness rates. The 15 off-diagonal terms of **K** must vanish. However, for a three-dimensional rigid-body system supported by 3 or 4 mounts, the complete dynamic decoupling of mounts is virtually impossible to achieve [11]. Therefore, only the partial decoupling is possible based on the focalization method [2, 7, 10]. It is presented in this paper and it will be compared with the proposed dynamic decoupling method. When a rigid body has a two plane symmetry or when it is represented in Γ_p, the cross-moments of inertia (I_{xy}, I_{xz}, and I_{yz}) vanish. Partial decoupling of physical modes, w_y, w_z, and θ_x may be achieved by placing four identical mounts in a symmetrical manner as shown in Figure 8 [7]. The physical projection of the elastic center of inclined mounts in the y–z plane onto the x-axis is mathematically achieved by forcing the element K_{24} of **K** (derived in Γ_p and given by equation (11)) to be zero. This leads to the relationship between the mount location parameter (a_y and a_z) and orientation angle (ϕ) and stiffness rates (k_p and $L = k_p/k_q$):

$$\frac{a_z}{a_y} = \frac{(L-1)\tan\phi}{L\tan^2\phi + 1}. \tag{41}$$

Equation (41) is graphically shown in Figure 9; it matches the results given in reference [2]. For a given stiffness ratio L, a_z/a_y should not exceed the following maximum value in order to

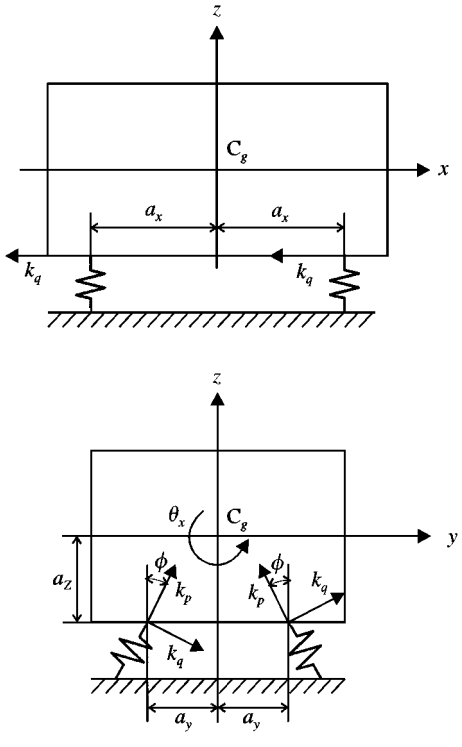

Figure 8. Focalization by the partial elastic axis decoupling method.

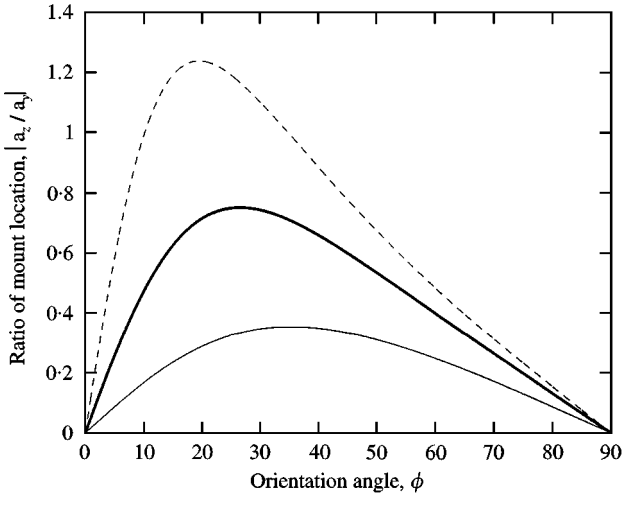

Figure 9. Design map for a symmetrical mounting system based on the focalization method. Key: —, $L = 2$; —, $L = 4$; – –, $L = 8$.

ensure the decoupling of elastic axis:

$$\left(\frac{a_z}{a_y}\right)_{\max} = \frac{L-1}{2\sqrt{L}} \quad \text{at} \quad \phi = \tan^{-1}\left(\frac{1}{\sqrt{L}}\right). \tag{42}$$

The natural frequency of the decoupled natural roll mode along θ_x is given by equation (37). Note that $y_0 + s_0 \cos\phi$ in equation (37) corresponds to a_y in Figure 8. This focalization method may also be applied to an asymmetrical inertial system in Γ_g provided cross-moments of inertia are small compared to I_{xx}. Examples of the next section will illustrate the focalization method using both Γ_p and Γ_g co-ordinate systems. Complete elastic axis decoupling of powertrain mounting system will also be attempted by minimizing the off-diagonal terms of stiffness matrix that is defined in the Γ_p co-ordinates.

9. EXAMPLES AND RESULTS

9.1. CONFIRMATION OF CLOSED-FORM SOLUTION: EXAMPLES I AND II

Two numerical examples for the mount-positioning scheme of Figure 5 are chosen to confirm the utility of the proposed method. System parameters are given in Table 1(a). From Table 1(b) observe that the proposed TRA mode decoupling approach works well as shown by the calculated eigenvector $\mathbf{u}_{TRA}$ for both examples. In particular, examine the displacement spectra for Example II there are shown in Figures 10–12. Only a dynamic range of 100 dB is shown in the spectra. The harmonic torque excitation $T(t)$ is parallel to the crankshaft axis and its amplitude is 100 N m over the range of frequencies. Directions of dynamic responses (w_x, w_y, w_z, θ_x, θ_y, and θ_z) are defined in the rigid-body inertial co-ordinate system (Γ_g) for Figure 10, in the principal inertial co-ordinate system (Γ_p) for Figure 11, and in the TRA co-ordinate system (Γ_{TRA}) for Figure 12. While the original mounting system and the elastic

TABLE 1

Examples I and II: simplified powertrain mounting systems

(a) System parameters

Mass	Example I $m = 50{\cdot}5$ kg	Example II $m = 73{\cdot}2$ kg
Moment of inertia (kg m^2)	$I_g = \begin{bmatrix} 1{\cdot}65 & 0 & 0 \\ 0 & 2{\cdot}43 & 0 \\ 0 & 0 & 2{\cdot}54 \end{bmatrix}$	$I_g = \begin{bmatrix} 1{\cdot}94 & -0{\cdot}129 & -0{\cdot}415 \\ -0{\cdot}129 & 3{\cdot}43 & 0{\cdot}073 \\ -0{\cdot}415 & 0{\cdot}073 & 3{\cdot}39 \end{bmatrix}$
Mount stiffness rates	$k_p = 8{\cdot}4 \times 10^5$ N/m; $L = 2{\cdot}5$	$k_p = 8{\cdot}4 \times 10^5$ N/m; $L = 2{\cdot}5$
Mount orientation	$\phi = 30^\circ$	$\phi = 30^\circ$

(b) Results

Example	f_{TRA} Hz	(a_{xi}, a_{yi}, a_{zi}) mm, i = mount index			
		$i = 1$	$i = 2$	$i = 3$	$i = 4$
I	38·3	(318, −198, −93·4)	(318, 198, −93·4)	(−318, −198, −93·4)	(−318, 198, −93·4)
II	29·8	(251, −173, −62·7)	(251, 182, −71·0)	(−251, −146, −78·3)	(−251, 144, −93·0)

Example	$\mathbf{u}_{TRA}$
I	$[4{\cdot}6 \times 10^{-18} \quad -9{\cdot}3 \times 10^{-17} \quad 8{\cdot}6 \times 10^{-16} \quad 1{\cdot}0 \quad -7{\cdot}6 \times 10^{-19} \quad 4{\cdot}6 \times 10^{-16}]^T$
II	$[2{\cdot}8 \times 10^{-17} \quad -1{\cdot}0 \times 10^{-17} \quad 8{\cdot}6 \times 10^{-16} \quad 1{\cdot}0 \quad -2{\cdot}6 \times 10^{-16} \quad -6{\cdot}1 \times 10^{-16}]^T$

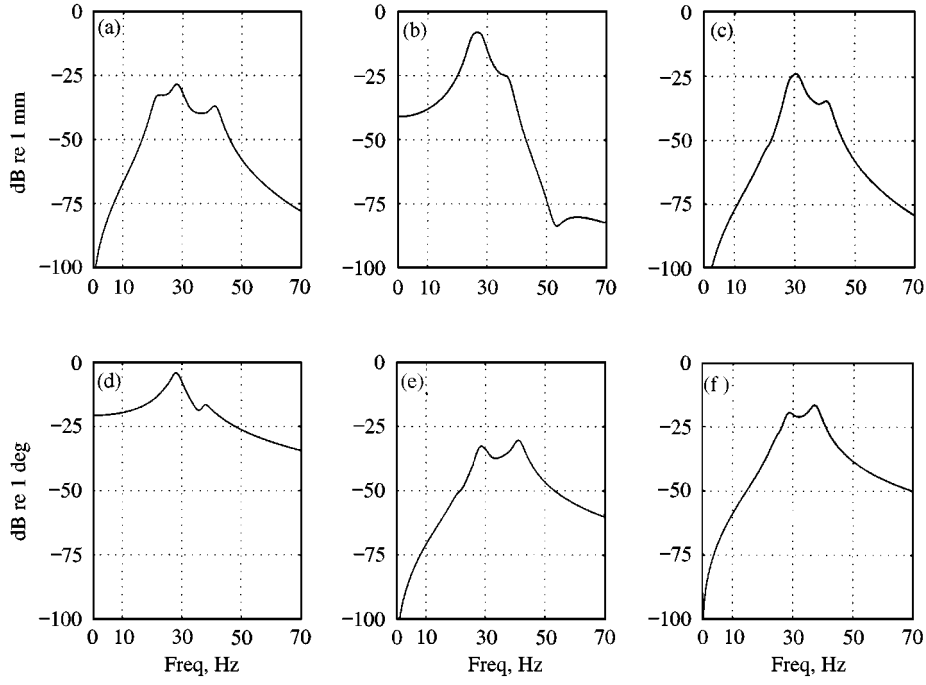

Figure 10. Displacement magnitude spectra of an asymmetric inertial system (Example II). These are for the original mounting system in Γ_g. (a) $|w_x|$, (*b*) $|w_y|$, (*c*) $|w_c|$, (*d*) $|\theta_x|$, (*e*) $|\theta_y|$, (f) $|\theta_z|$.

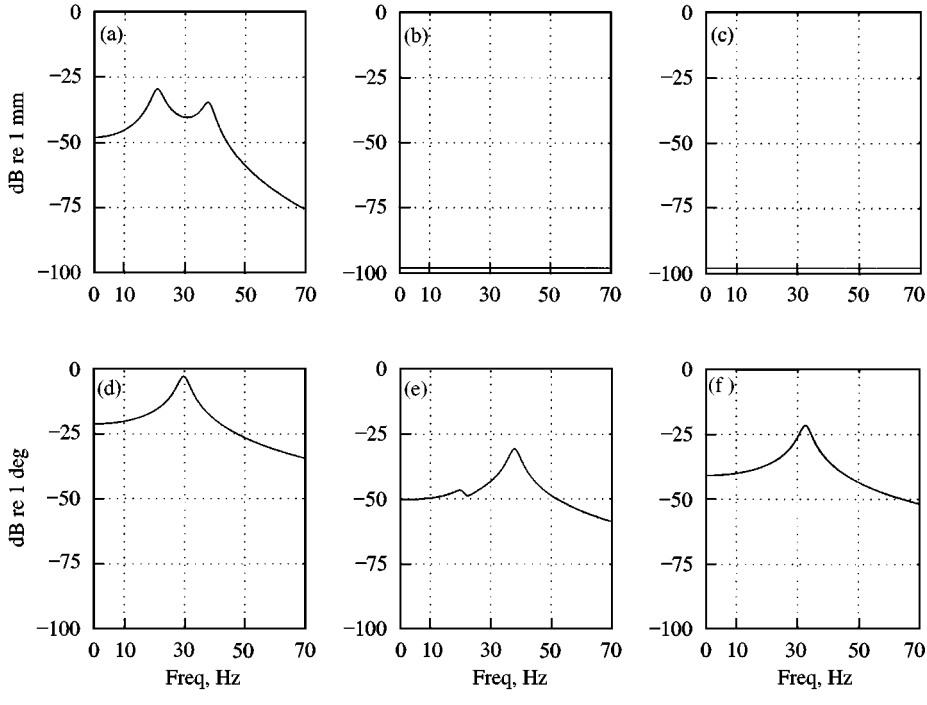

Figure 11. Displacement magnitude spectra of an asymmetric inertial system (Example II). These are for the elastic axis mounting system in Γ_p (focalized by partially decoupling). (a) $|w_x|$, (b) $|w_y|$, (c) $|w_c|$, (d) $|\theta_x|$, (e) $|\theta_y|$, (f) $|\theta_z|$.

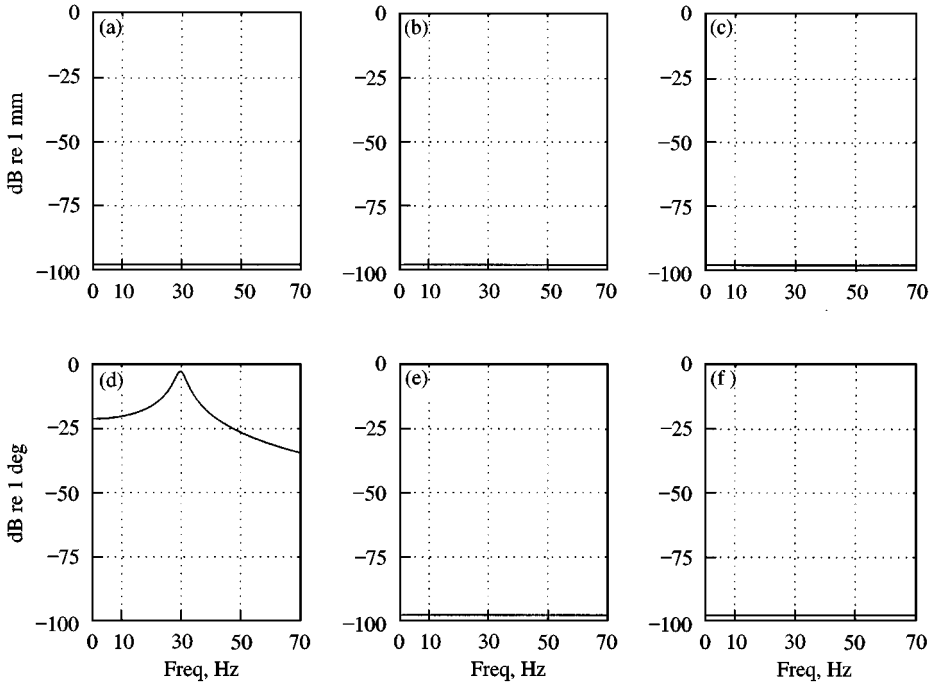

Figure 12. Displacement magnitude spectra of an asymmetric inertial system (Example II). These are for the TRA mode-decoupled mounting system in Γ_{TRA}. (a) $|w_x|$, (b) $|w_y|$, (c) $|w_z|$, (d) $|\theta_x|$, (e) $|\theta_y|$, (f) $|\theta_z|$.

axis mounting strategy produce non-negligible responses in several directions, the proposed method shows a true decoupling of the TRA mode, which is parallel to the x-axis in Γ_{TRA}. These examples confirm the utility of the new axiom and the closed-form solution.

9.2. PARAMETRIC STUDIES: EXAMPLE II

The results of a typical parametric study are shown in Figure 13. Three parameters have been selected to illustrate the design concepts: orientation angle ϕ, stiffness ratio $L = k_p/k_q$, and principal compressive stiffness value k_p. Their effects are quantified in terms of the natural frequency of the decoupled TRA mode f_{TRA}. All parameters and results are non-dimensionalized by using the values of Example II (given Tables 1) as reference (*ref*):

$$f^*_{TRA} = \frac{f_{TRA}}{f_{TRA,ref}}, \quad \phi^* = \frac{\phi}{\phi_{ref}}, \quad L^* = \frac{L}{L_{ref}}, \quad k^*_p = \frac{k_p}{k_{p,ref}}. \tag{43}$$

Design guidelines are clearly depicted in Figure 13. For example, when f_{TRA} is decreased further to provide improved vibration isolation at lower speeds including the idling condition, one needs to reduce ϕ and L since they are almost inversely proportional to f_{TRA}. Even though the results of Figure 11 are generated by varying one parameter at a time, two parameters may be simultaneously changed producing a 3-D design map, which will be very helpful especially in the early stages of design.

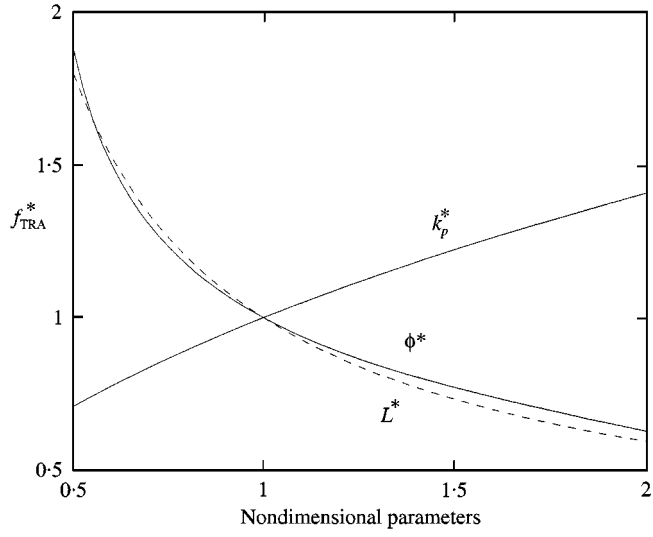

Figure 13. Effect of design parameters on the decoupled TRA mode natural frequency (Example II).

TABLE 2

Example III: original mounting system of V-6 diesel engine [9]

Mass	*Moment of inertia* (kg m^2)
$m = 276{\cdot}70$ kg	$\mathbf{I}_g = \begin{bmatrix} 11{\cdot}64 & -0{\cdot}8 & 3{\cdot}2 \\ -0{\cdot}8 & 15{\cdot}8 & 0{\cdot}9 \\ 3{\cdot}2 & 0{\cdot}9 & 15{\cdot}69 \end{bmatrix}$

Mount #	Stiffness (N/m)		
	Compression, k_p	Lateral, k_q	Fore-aft, k_r
1	223 667	44 733	44 733
2	170 167	126 050	48 619
3	217 167	434 334	108 583
4	232 167	464 334	116 083

Mount #	Mount orientation (deg)		
	φ_x	φ_y	φ_z
1	0	−45	0
2	0	−39	180
3	0	−75	0
4	0	−45	180

9.3. COMPARISON WITH LITERATURE: EXAMPLE III

The next example Example III considers the mounting parameters for a V-6 diesel engine as listed in Table 2. This case was considered by Spiekermann *et al.* [9]. They had simulated the engine mounting system and its was validated by comparing predictions with a modal

TABLE 3

Modal analysis of Example III

(a) Natural frequencies

Natural mode		1st	2nd	3rd	4th	5th	6th
Computer	Our method	4·473	5·971	7·479	9·872	12·266	16·452
Simulation	Spiekermann *et al.* [9]	4·47	5·97	7·48	9·87	12·26	16·46
Experiment [9]		4·17	5·66	6·47	8·76	12·47	N/A

(b) Natural mode shapes from computer simulation

	Natural mode	1st	2nd	3rd	4th	5th	6th
x	Our method	0·300	0·107	0·057	− 0·018	− 0·117	− 0·178
	Spiekermann *et al.*	0·300	0·107	0·058	− 0·108	− 0·117	− 0·180
y	Our method	0·081	− 0·414	0·134	0·094	− 0·077	0·018
	Spiekermann *et al.*	0·080	− 0·414	0·137	0·093	− 0·078	0·018
z	Our method	− 0·029	0·049	1·000	− 0·004	0·029	− 0·005
	Spiekermann *et al.*	− 0·029	0·050	1·000	− 0·004	0·029	− 0·005
θ_x	Our method	− 0·163	1·000	0·012	1·000	− 0·706	0·490
	Spiekermann *et al.*	− 0·163	1·000	0·015	1·000	− 0·708	0·491
θ_y	Our method	1·000	0·220	0·019	0·133	0·607	1·000
	Spiekermann *et al.*	1·000	0·220	0·021	0·134	0·609	1·000
θ_z	Our method	− 0·019	− 0·194	− 0·244	0·391	1·000	− 0·984
	Spiekermann *et al.*	− 0·019	− 0·195	− 0·243	0·392	1·000	− 0·987

experiment; key results are shown in Table 3. Our method is compared with prior modal solutions in Table 3. Here the amplitude of the pulsating torque is 200 N m.

9.4. COMPARATIVE EVALUATION OF MOUNTING METHODS: EXAMPLES III AND IV

Figures 14 and 15 compares the displacement spectra corresponding to the original engine mounting, the optimized design of Spiekermann *et al.* [9], and the focalized mounting concept; relevant parameters of Example III are listed in Tables 2 and 4. All mounting system designs are described in Γ_g. Since the main objective in the earlier optimization [9] was to ensure that the rigid-body vibration modes do not fall within the undesirable frequency band, they could not decouple the physical modes. In contrast, the focalized engine mounting concept (as presented in this article) decouples the physical modes between θ_x, w_y, and w_z. However, this particular method still does not decouple other physical modes. Even the elastic axis decoupling method (focalization in Γ_p via partial elastic axis decoupling) produces non-negligible responses in w_x, θ_y, and θ_z as shown in Figure 16. Both focalizations produce the same degree of decoupling. While the focalization in Γ_p has only one peak in the physical roll mode, the one in Γ_g has two peaks. However, if one considers the mount locations of Figures 18 and 19, one may conclude that a simple focalization in Γ_g is more feasible than the one in Γ_p. Figure 17 confirms that only the TRA mode decoupling achieves a complete decoupling of physical modes.

Consider the final example (Example IV) based on the minimization of the off-diagonal terms of stiffness matrix in Γ_p to achieve a complete elastic axis decoupling using the MATLAB based algorithm [16]. Initial values for the minimization are taken from Example III;

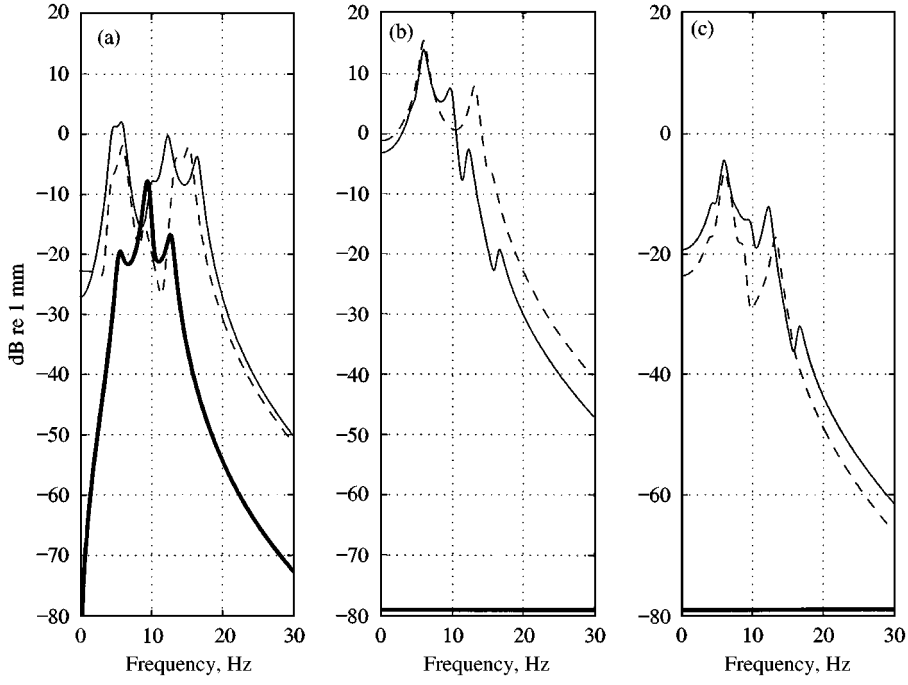

Figure 14. Comparison of translational displacement magnitude spectra between three different engine mounting schemes (Example III). Key: —, original mounting system [9]; – –, optimized mounting system [9]; ▬, focalized mounting system in Γ_g. (a) $|w_x|$, (b) $|w_y|$, (c) $|w_z|$.

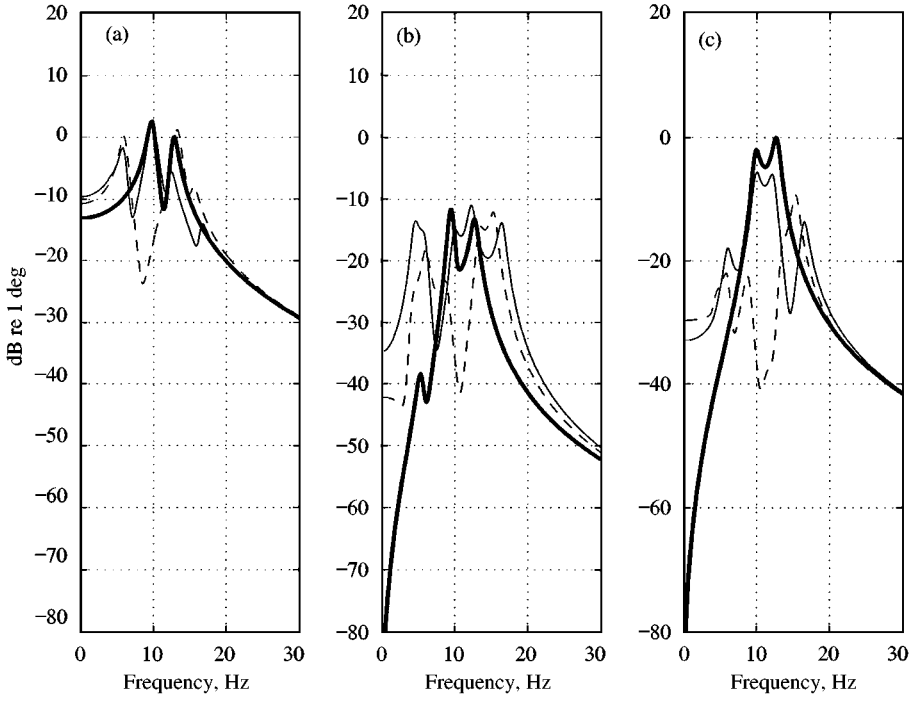

Figure 15. Comparison of rotational displacement magnitude spectra between three different engine mounting schemes (Example III). Key: —, original mounting system [9]; – –, optimized mounting system [9]; ▬, focalized mounting system in Γ_g. (a) $|\theta_x|$, (b) $|\theta_y|$, (c) $|\theta_z|$.

TABLE 4

Comparison of TRA decoupling methods for Example III

Parameters	Focalization in Γ_g	Focalization in Γ_p	TRA decoupling in Γ_{TRA}
Mount stiffness rates	$k_p = 2{\cdot}5 \times 10^5$ N/m $L = 2{\cdot}5$	$k_p = 2{\cdot}5 \times 10^5$ N/m $L = 2{\cdot}5$	$k_p = 2{\cdot}5 \times 10^5$ N/m $L = 2{\cdot}5$
Mount orientation	$\phi = 45^\circ$	$\phi = 45^\circ$	$\phi = 55^\circ$

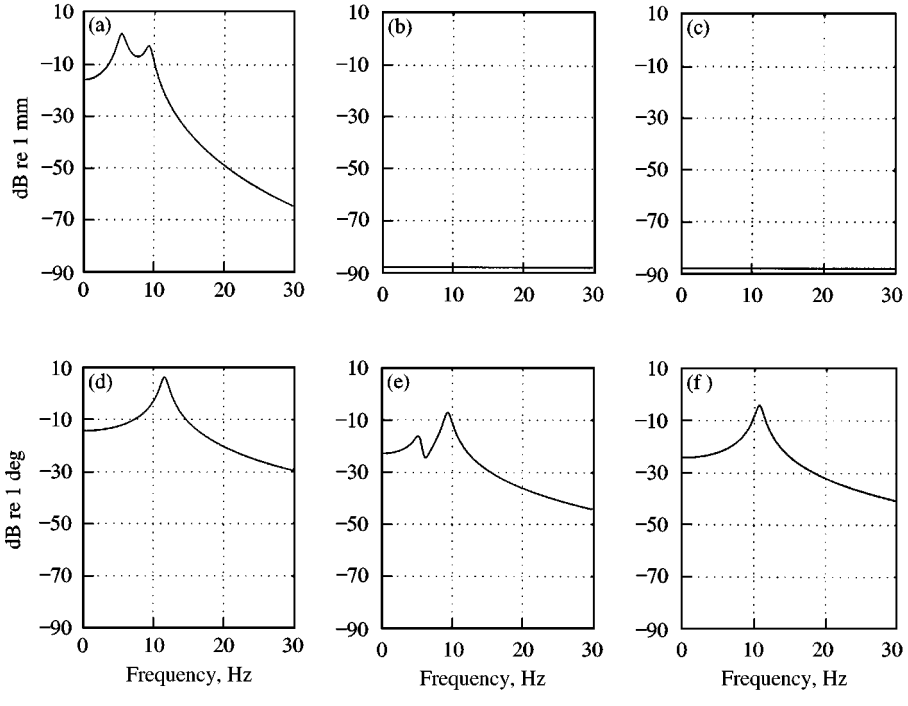

Figure 16. Displacement magnitude spectra of the focalized (partial elastic axis decoupling) engine mounting system in Γ_p for Example III. (a) $|w_x|$, (b) $|w_y|$, (c) $|w_z|$, (d) $|\theta_x|$, (e) $|\theta_y|$, (f) $|\theta_z|$.

the mount locations in the original mounting system, the mount orientations and stiffness rates in the focalized mounting system. Results are shown in Table 5. Note that the orientation angle is defined by the Eulerian angles ϕ_{ui} [17]. Based on the minimized stiffness matrix of Table 5(b), the calculated mode shapes, as shown in Table 5(c), show a virtually decoupled mounting system using the elastic axis mounting method. Finite responses along θ_y and θ_z, as shown in Figure 20, are due to the projected torque components (of $T_x(t)$ in Γ_g) around the y- and z-axis in Γ_p. Mount locations of Example IV are shown in Figure 21; note that significant changes in the locations are necessary to decouple the powertrain.

10. CONCLUSION

A new axiom for the TRA mode decoupling has been suggested and the necessary mathematical conditions have been established. Computer simulations confirm the findings

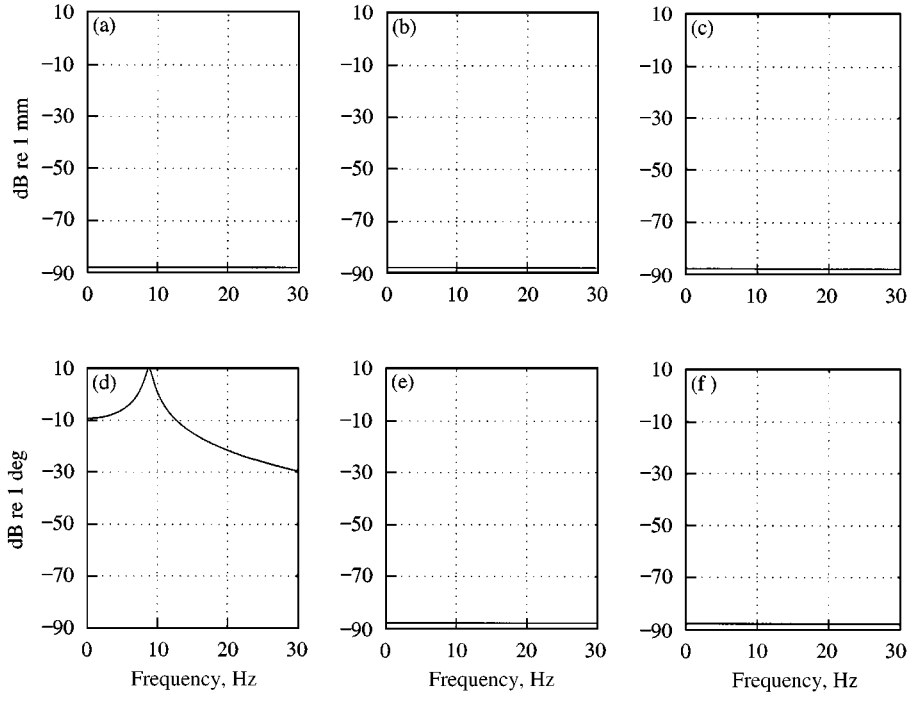

Figure 17. Displacement magnitude spectra of the TRA decoupled engine mount system in Γ_{TRA} for Example III. (a) $|w_x|$, (b) $|w_y|$, (c) $|w_z|$, (d) $|\theta_x|$, (e) $|\theta_y|$, (f) $|\theta_z|$.

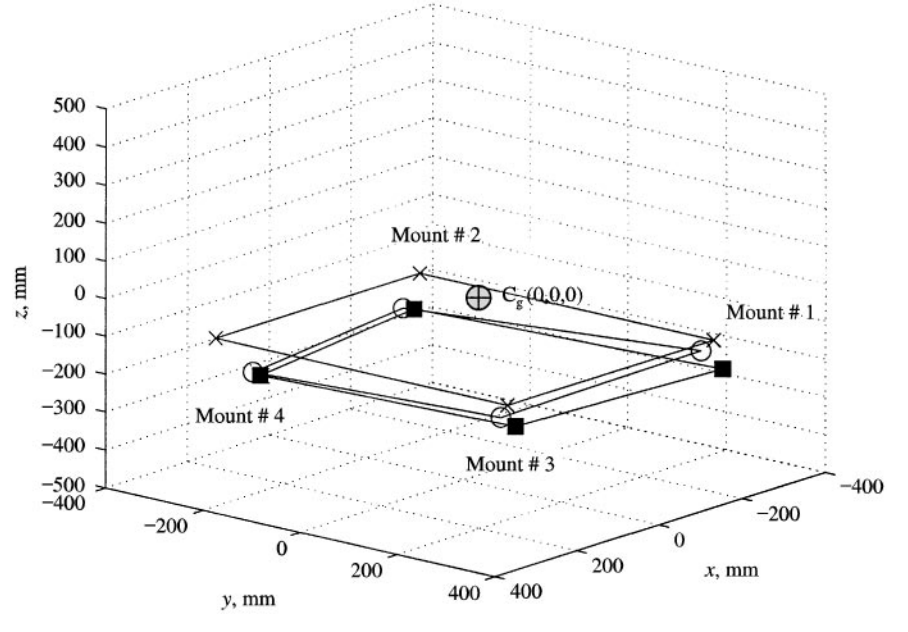

Figure 18. Location of mounts in Γ_g for Example III. ○, original mounting; ■, optimized mounting; ×, focalized mounting in Γ_g. The origin is at C_g. Also compare this sketch with Figure 19.

TABLE 5

Example IV: *elastic axis decoupling by minimizing the off-diagonal terms of stiffness matrix in* Γ_p

(a) Stiffness rates and orientation angles

Mount #	Stiffness (N/m)		
	Compression, k_p	Lateral, k_q	Fore-aft, k_r
1	426 870	207 470	147 790
2	347 590	182 370	114 400
3	224 710	265 710	126 250
4	314 550	159 470	140 860

Mount #	Mount orientation: Euler angles (deg.)		
	ϕ_{u1}	ϕ_{u2}	ϕ_{u3}
1	162·8	− 117·9	40·92
2	− 141·6	− 127·7	− 4·520
3	90·65	− 52·35	− 16·01
4	− 144·0	− 60·24	− 2·669

(b) Stiffness matrix

$$\mathbf{K} = \begin{bmatrix} 7{\cdot}11 & 1{\cdot}26\times10^{-6} & -4{\cdot}97\times10^{-7} & -2{\cdot}32\times10^{-7} & -1{\cdot}89\times10^{-5} & 3{\cdot}50\times10^{-6} \\ & 9{\cdot}32 & 1{\cdot}60\times10^{-6} & 1{\cdot}04\times10^{-5} & -1{\cdot}41\times10^{-5} & -2{\cdot}44\times10^{-6} \\ & & 1{\cdot}02 & -5{\cdot}02\times10^{-6} & -6{\cdot}21\times10^{-7} & 2{\cdot}46\times10^{-7} \\ & & & 6{\cdot}87 & -8{\cdot}10\times10^{-7} & -7{\cdot}64\times10^{-6} \\ & & & & 0{\cdot}456 & 1{\cdot}32\times10^{-5} \\ & & & & & 0{\cdot}912 \end{bmatrix} \times 10^5 \text{ N/m}$$

(c) Natural frequencies and mode shapes

Natural mode	1st 8·07 Hz	2nd 8·52 Hz	3rd 9·24 Hz	4th 9·64 Hz	5th 11·5 Hz	6th 13·4 Hz
x	**1·0000**	$-2{\cdot}3\times10^{-5}$	$5{\cdot}7\times10^{-7}$	$-1{\cdot}6\times10^{-7}$	$4{\cdot}8\times10^{-7}$	$-1{\cdot}9\times10^{-8}$
y	$-5{\cdot}7\times10^{-7}$	$1{\cdot}0\times10^{-8}$	**1·0000**	$1{\cdot}9\times10^{-6}$	$-4{\cdot}8\times10^{-7}$	$1{\cdot}0\times10^{-6}$
z	$1{\cdot}6\times10^{-7}$	$2{\cdot}8\times10^{-7}$	$-1{\cdot}9\times10^{-6}$	**1·0000**	$5{\cdot}8\times10^{-8}$	$-5{\cdot}3\times10^{-7}$
θ_x	$5{\cdot}3\times10^{-7}$	$2{\cdot}0\times10^{-6}$	$-2{\cdot}9\times10^{-5}$	$1{\cdot}5\times10^{-5}$	$4{\cdot}1\times10^{-5}$	**1·0000**
θ_y	$4{\cdot}0\times10^{-4}$	**1·0000**	$-1{\cdot}8\times10^{-7}$	$-4{\cdot}9\times10^{-6}$	$3{\cdot}6\times10^{-5}$	$-1{\cdot}2\times10^{-6}$
θ_z	$-7{\cdot}6\times10^{-6}$	$-3{\cdot}2\times10^{-5}$	$7{\cdot}6\times10^{-6}$	$-9{\cdot}2\times10^{-7}$	**1·0000**	$-2{\cdot}3\times10^{-5}$

and demonstrate that only the TRA mode decoupled engine mounting scheme provides a complete decoupling of physical modes. When a powertrain has small cross-moment of inertia terms compared with the diagonal terms, the focalization in Γ_g is found to be better than the one in Γ_p. Based on the results of this paper, key features of the competing mounting methods, and characteristics of mounting methods are summarized in Table 6. When compared with the original mounting locations, the TRA-mounting scheme and the

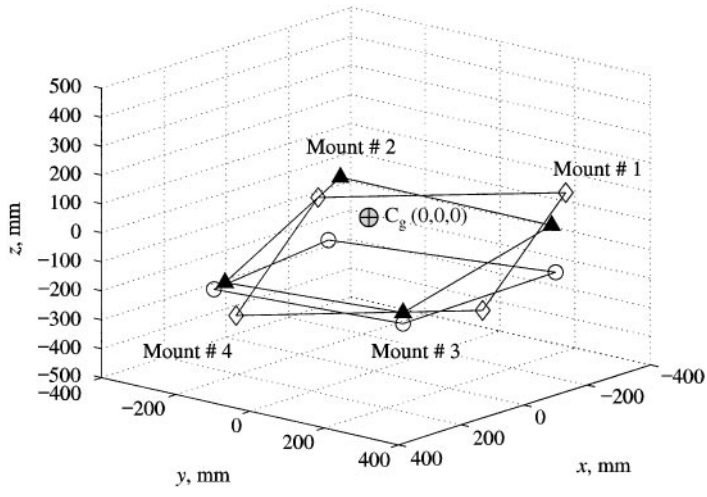

Figure 19. Location of mounts in Γ_g for Example III. ○, original mounting; ◇, focalized mounting in Γ_p; ▲, TRA decoupled in Γ_{TRA}. The origin is at C_g. Also compare this sketch with Figure 18.

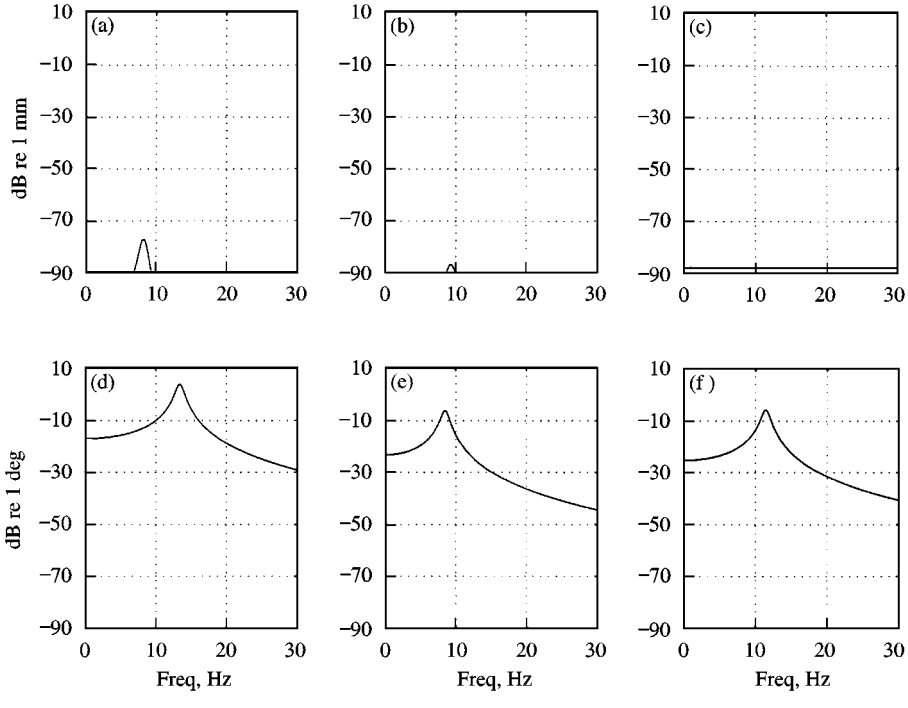

Figure 20. Displacement magnitude spectra of the minimized elastic axis engine mounting system in Γ_p for Example IV. (a) $|w_x|$, (b) $|w_y|$, (c) $|w_z|$, (d) $|\theta_x|$, (e) $|\theta_y|$, (f) $|\theta_z|$.

minimized elastic-axis-mounting scheme show a significant change in the locations of mounts #1 and #2. Also recall from the closed-form solution developed for a simplified mounting scheme, the restriction p_{zi}, $i = 1$–4, to be $-z_0$. Such a restriction may cause one pair of mounts to be located rather too high compared with the original mount positions. In general, an optimization algorithm is needed to restrict the location and the orientation of

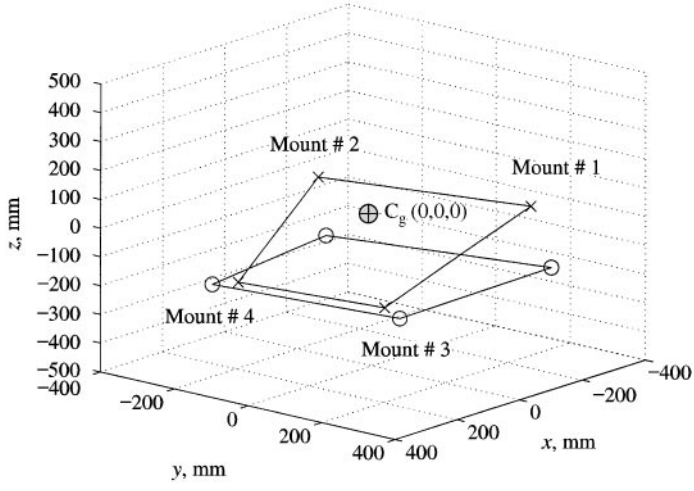

Figure 21. Location of mounts in Γ_g for Example IV. ○, original mounting; ×; minimized elastic axis mounting in Γ_p.

TABLE 6

Comparison of TRA decoupling methods

		Focalization method	Partial elastic axis decoupling method	TRA decoupling method
Co-ordinate system to be chosen		Γ_g (rigid-body inertial)	Γ_p (principal inertial)	Γ_{TRA} axes)
Applicable to		Symmetric system or almost symmetric system	Asymmetric system	Asymmetric system
Equations of motions	Mass matrix	Diagonal or almost diagonal	Diagonal	Non-diagonal
	Damping matrix	Proportional damping	Proportional damping	Proportional damping
	Stiffness matrix	Diagonal except the coupling term between w_x and θ_y	Diagonal except the coupling term between w_x and θ_y	Non-diagonal
Concept		Place the elastic center of inclined mounts on the roll axis assuming that the rigid-body system has two planes of symmetry	Place the elastic center of inclined mount on the roll axis. Or minimize the off-diagonal terms of stiffness matrix	Force the total mount reaction forces to cancel out and induce the total mount reaction moment to be parallel to the excitation torque. Hence produce pure rotation only about the TRA axis
Dynamic response		When the powertrain has negligible cross moment of inertia, it decouples physical modes between w_y, w_z, and θ_x	Decouples physical modes between w_y, w_z, and θ_x.	The TRA mode is completely decoupled with other physical modes.

mounts and to ensure that the natural frequencies of the engine rigid-body modes lie within the desirable band while maintaining the decoupled TRA mode. This work is beyond the scope of this paper.

Future study may also include modifications to the closed-form solutions, which should remove some of the constraints in selecting the origins of mounting co-ordinates. In addition, the effect of frequency- and amplitude-dependent mount properties, and the influence of compliant body/chassis on the mounting system should be considered [1, 3, 14, 15].

ACKNOWLEDGMENT

The Chrysler Challenge Fund and the Goodyear Tire and Rubber Company (St. Marys) are gratefully acknowledged for supporting this research.

REFERENCES

1. G. KIM and R. SINGH 1995 *Journal of Sound and Vibration* **179**, 427–453. A study of passive and adaptive hydraulic engine mount systems with emphasis on non-linear characteristics.
2. S. R. RACCA 1982 *SAE Technical Paper Series* 821095. How to select power-train isolators for good performance and long service life.
3. T. ROYSTON and R. SINGH 1996 *Journal of Sound and Vibration* **194**, 295–316. Optimization of passive and active nonlinear vibration mounting systems based on vibratory power transmission.
4. F. F. TIMPNER 1965 *SAE Technical Paper Series* 650093 (966B). Design considerations for engine mounting.
5. P. E. GECK and R. D. PATTON 1984 *SAE Technical Paper Series* 840736. Front wheel drive engine mount optimization.
6. R. M. BRACH 1997 *SAE Technical Paper Series* 971942. Automotive powerplant isolation strategies.
7. C. M. HARRIS 1995 *Shock and Vibration Handbook*. New York: McGraw-Hill, Chapter 3, third edition.
8. J. E. BERNARD and J. M. STARKEY 1983 *SAE Technical Paper Series* 830257. Engine mount optimization.
9. C. E. SPIEKERMANN, C. J. RADCLIFFE and E. D. GOODMAN 1985 *Transactions of ASME, Journal of Mechanisms, Transmissions, and Automation in Design* **107**, 271–276. Optimal design and simulation of vibrational isolation systems.
10. D. FITZGERALD 1997 *Korfund Dynamics, Co. Application Note*. Focused engine isolation systems—the benefits.
11. B. J. KIM 1991 *M. S. thesis, Michigan State University*. Three dimensional vibration isolation using elastic axes.
12. T. F. DERBY 1973 *Shock and Vibration Bulletin*, Part 4 **43**, 91–108. Decoupling the three translational modes from the three rotational modes of a rigid body supported by four corner-located isolators.
13. D. M. FORD 1985 *SAE Technical Paper Series* 850976. An analysis and application of a decoupled engine mount systems for idle isolation.
14. H. ASHRAFIUON 1993 *Transactions of ASME, Journal of Vibration and Acoustics* **115,** 463–467. Design optimization of aircraft engine-mount systems.
15. T. ROYSTON and R. SINGH 1997 *Journal of Acoustical Society of America* **101**, 2059–2069. Vibratory power flow through a nonlinear path into a resonant receiver.
16. The mathworks Matlab 5.3. Optimization Tool Box.
17. H. GOLDSTEIN 1950 *Classical Mechanics*. Cambridge MA: Addison-Wesley, Chapter 4.

APPENDIX A: DEFINITION OF THE DIRECTION

To define the TRA direction, consider the Euler's equations of motion when a harmonic torque $T_x(t) = T_{xa}e^{i\omega t}$ is applied about the x-axis:

$$\mathbf{M}_\theta \ddot{\boldsymbol{\theta}}_g(t) + \dot{\boldsymbol{\theta}}_g(t) \otimes \mathbf{M}_\theta \dot{\boldsymbol{\theta}}_g(t) = [T_{xa} \;\; 0 \;\; 0]^{\mathrm{T}} e^{i\omega t}, \tag{A1}$$

where $\mathbf{M}_\theta$ is defined in equation (2), $\otimes$ is the vector product, and $\boldsymbol{\theta}_g$ is defined in equation (1). Since the rotational displacements are assumed to be small, the term $\dot{\boldsymbol{\theta}}_g \otimes \mathbf{M}_\theta \dot{\boldsymbol{\theta}}_g$ is negligible. Hence the response $\boldsymbol{\theta}_g(t)$, which is the rotation about the TRA, will be $-\mathbf{M}_\theta^{-1}[T_a \ 0 \ 0]^{\mathrm{T}} e^{i\omega t}/\omega^2$. This results in the unique TRA direction $\boldsymbol{\theta}_{TRA}$ as follows:

$$\boldsymbol{\theta}_{TRA} = a\mathbf{M}_\theta^{-1}[1 \ 0 \ 0]^{\mathrm{T}}, \tag{A2}$$

where a is normalizing constant for the first column of $\mathbf{M}_\theta^{-1}$. One can define the TRA direction in the Γ_g co-ordinate system by using equation (A2) as

$$\mathbf{q}_{TRA} = [0 \ 0 \ 0 \ \boldsymbol{\theta}_{TRA}^{\mathrm{T}}]^{\mathrm{T}}, \tag{A3}$$

For an arbitrary torque $\mathbf{T}(t) = \mathbf{T}_a e^{i\omega t} = [0 \ 0 \ 0 \ T_{xa} \ T_{ya} \ T_{za}]^{\mathrm{T}} e^{i\omega t}$, the TRA direction $\mathbf{q}_{TRA}$ is obtained as follows where b is a suitable normalizing constant:

$$\mathbf{q}_{TRA} = b\mathbf{M}^{-1}\mathbf{T}_a. \tag{A4}$$

APPENDIX B: NOMENCLATURE

a, b, c, d	arbitrary scalar constant or coefficient
a_x, a_y, a_z	distance of mount from C_g in x, y, and z directions
a_{xi}, a_{yi}, a_{zi}	co-ordinates of the ith mounting point
$a(\omega), b(\omega), c(\omega)$	spectral functions
$\mathbf{B}$	rotation matrix for the cross-vector product
$\mathbf{C}$	viscous damping matrix
$\mathbf{C}_g$	center of gravity
f_{TRA}	natural frequency of the TRA mode
$\mathbf{f}$	external force vector
$\mathbf{H}$	structural damping matrix
i	$\sqrt{-1}$
I	moment of inertia
$\mathbf{I}$	identity matrix
J	matrix element of $\mathbf{J}$
$\mathbf{J}$	inverse of moment of inertia matrix
k	stiffness
k_p, k_q, k_r	principal stiffnesses
k_t	torsional stiffness
$\mathbf{K}$	stiffness matrix
L	stiffness ratio (k_p/k_q)
m	mass
$\mathbf{M}$	inertia matrix
N	dimension of a dynamic system
r_c	characteristic dimension of mount
$\mathbf{r}$	position vector in the geometric co-ordinates
$\mathbf{R}$	reaction force vector
$\mathbf{P}_i$	origin of Γ_{mi}
(P_{xi}, P_{yi}, P_{zi})	co-ordinates of $\mathbf{P}_i$ in Γ_{TRA}
$\mathbf{q}$	generalized displacement vector
$\mathbf{q}_{TRA}$	torque roll axis vector
t	time
T	torque amplitude
$\mathbf{T}$	torque vector
$\mathbf{u}$	eigenvector of dimension N
w	translational displacement
$\mathbf{w}$	translational displacement vector of dimension 3

x, y, z	geometric co-ordinates in Γ_g or Γ_{TRA}
x', y', z'	geometric co-ordinates in Γ_{TRA}
x_e, y_e, z_e	geometric co-ordinates in Γ_e
x_p, y_p, z_p	geometric co-ordinates in Γ_p
x_{si}, y_{si}, z_{si}	geometric co-ordinates in Γ_{si}
s_i, ϕ_i	geometric co-ordinate in Γ_{mi}
Γ_e	principal elastic axis co-ordinate system
Γ_g	rigid-body inertial co-ordinate system with origin at C_g
Γ_{mi}	mounting co-ordinate system for the ith mount
Γ_p	principal inertial co-ordinate system
Γ_{si}	principal elastic co-ordinate system of the ith mount
Γ_{TRA}	torque roll axis co-ordinate system
ϕ	orientation angle of mount
ϕ_{ui}	ith Eulerian angle
λ	eigenvalue
$\mathfrak{R}$	rotational transformation matrix
θ	rotational displacement
$\boldsymbol{\theta}$	rotational displacement vector of dimension 3
ω	frequency, rad/s
v	directional cosine
$\boldsymbol{\Pi}$	transformation matrix

Subscripts

a	amplitude
e	Γ_e co-ordinate system
g	Γ_g co-ordinate system
$i = 1, 2, 3, 4$	mount index
$j, r = 1, 2, \ldots, N$	modal indices
p	Γ_p co-ordinate system
p, q, r	principal stiffness directions
si	Γ_{si} co-ordinate system for the ith mount
ui	ith Eulerian angle
w	translational direction
TRA	torque roll axis direction or (Γ_{TRA})
x, y, z	Cartesian co-ordinates
θ	rotational direction

Superscripts

T	transpose

Operators

diag	diagonal matrix